Pergamon

Int. J. Heat Mass Transfer. Vol. 37, No. 14, pp. 2017–2024, 1994

0017-9310/94 $7.00+0.00

0017-9310(94)E0044-U

Development of thermal stratification in a two-dimensional cavity: a numerical study

MOHAMED JOMAA SAFI
E.N.I.T., B.P 37, Belvèdère 1002 Tunis, Tunisia

and

TA PHUOC LOC†
L.I.M.S.I, BP 133, F 91403 Orsay Cedex, France

(*Received for publication* 11 *February* 1994)

Abstract—A numerical study of the thermal stratification in an open cavity with one heated discharge is carried out. The inflow by a slot is located at the top of one vertical wall of the cavity and outflow occurs at the opposite wall. The two-dimensional flow is described by the Navier–Stokes and the energy equations. A finite difference scheme is used to solve these partial differential equations. The influence of non-dimensional parameters (Reynolds, Peclet and Richardson numbers) on the flow behavior and the stratification is examined.

1. INTRODUCTION

IN SOME industrial applications, such as the cooling of the thermoelectric generating stations, it is desirable to keep the hot and cold fluids separated without requiring physical action. This phenomena, called stratification, is also often employed for improving the efficiency of the collection and storage system [1, 2]. The first example, where the medium is water with a free surface, has been discussed by Abraham [3] and Hart [4] who proposed analytical models, and by Urban [5] who studied experimentally the stability of the flow.

In the second example the fluid was confined by rigid walls with inflows set at various positions. Jaluria and Gupta [6] studied experimentally and numerically the thermal stratification resulting from a heated discharge at the middle of one side of a cavity while the exit varied along the opposite side. Their numerical investigations were limited to $Re = 50$ and $Ri = 1$. Cabelli [2] has carried out a numerical study of the flow and temperature fields in a thermal storage tank for $Re = 100$ and 200, $Gr = 10^3$ and 10^4 and $Pr = 2$. His tank included horizontal and vertical entries. When the incoming flow is horizontal, the outflow is set on the same side, so no comparisons could be made with the previous work. Oberkampf and Crow [7] tested a rectangular reservoir where the inflow is allowed horizontally at the surface on one end and outflow occurs at any depth on the opposite end. Their numerical simulations were performed for $Re = 10^4$, $Pr = 5$ and Gr approximately 10^{12}, assuming a laminar flow.

In spite of different geometries and adimensional parameter values used in previous works, we can conclude that:

(a) the stratification can occur in a cavity since $Ri = 1$ and for all aspect ratio values; and
(b) current reversals occur against the wall upon the exit even when the incoming flow is parallel to the gravity vector.

The present work deals with a hot laminar jet which enters horizontally into a square cavity at the top of one end: the exit occurs at the bottom of the opposite side. This geometry is known to allow the best stratification [8]. The small size of the inlet (or the outlet) with regard to the depth cavity was chosen to have the same magnitude as the size diffusers used in the industry. The study is focused on two points:

(1) the understanding of the basic mechanism that arises when the stratification occurs by following the time evolution of the flow pattern; and
(2) the effect of non-dimensional parameters on the fluid dynamic and the stratification.

2. PHYSICAL PROBLEM AND GOVERNING EQUATIONS

We consider a laminar jet of incompressible viscous fluid which enters into the cavity by (1) and exits by (2) (Fig. 1). The equations which describe the motion are those expressing the conservation of mass,

†Author to whom correspondence should be addressed.

NOMENCLATURE

C_P	specific heat at constant pressure
g	gravitational constant
H	cavity depth
h	space step
h_e	exit width
h_0	inlet width
L	cavity length
T	dimensional temperature
t	time
T^0	temperature at $t = 0$
ΔT	temperature difference $T_0 - T^0$
U_0	reference speed at the inlet
u, v	velocities in the x and y directions
x, y	co-ordinate system
$\Delta X, \Delta Y$	mesh sizes in the x and y directions.

Dimensionless parameters

Gr	Grashof number, $g\beta\Delta TH^3/\nu_0^2$
Pe	Peclet number, Pr^*Re
Pr	Prandtl number, $\mu c_p/\lambda$
Ra	Rayleigh number, Gr^*Pr
Re	Reynolds number, U_0H/ν_0
Ri	Richardson number, Gr/Re^2.

Greek symbols

θ	adimensional temperature
λ	thermal conductivity
μ	absolute viscosity
ν	kinematics viscosity, μ/ρ
ξ	vorticity
ρ	mass density
τ_x, τ_y	optimum coefficients of relaxation in x and y directions
ψ	stream function.

Subscripts

0	inlet
e	exit
el	one point in front of the exit
i, j	mesh point (i, j)
p	wall.

Superscripts

$'$	dimensional quantity
k	time level k of numerical integration
n	time level of numerical integration.

momentum and energy. The following assumptions are made:

(a) the fluid is Newtonian;
(b) the motion is two-dimensional; and
(c) the physical properties of the fluid are constant except for density variations which affect the buoyancy force only (Boussinesq approximation).

Then the equations describing this motion are the stream function, vorticity transport equation and energy equation:

$$\frac{\partial^2\psi}{\partial x^2} + \frac{\partial^2\psi}{\partial y^2} = \xi \tag{1}$$

$$\frac{\partial}{\partial t}\xi + \frac{\partial}{\partial x}u\xi + \frac{\partial}{\partial y}v\xi = \frac{1}{Re}\left(\frac{\partial^2\xi}{\partial x^2} + \frac{\partial^2\xi}{\partial y^2}\right) + Ri\frac{\partial\theta}{\partial x} \tag{2}$$

$$\frac{\partial\theta}{\partial t} + \frac{\partial u\theta}{\partial x} + \frac{\partial v\theta}{\partial y} = \frac{1}{Pe}\left(\frac{\partial^2\theta}{\partial x^2} + \frac{\partial^2\theta}{\partial y^2}\right), \tag{3}$$

with:

$$u = -\frac{\partial\psi}{\partial y} \quad v = \frac{\partial\psi}{\partial x} \quad \xi = \frac{\partial}{\partial x}v - \frac{\partial}{\partial y}u.$$

These equations have been non-dimensionalized by defining:

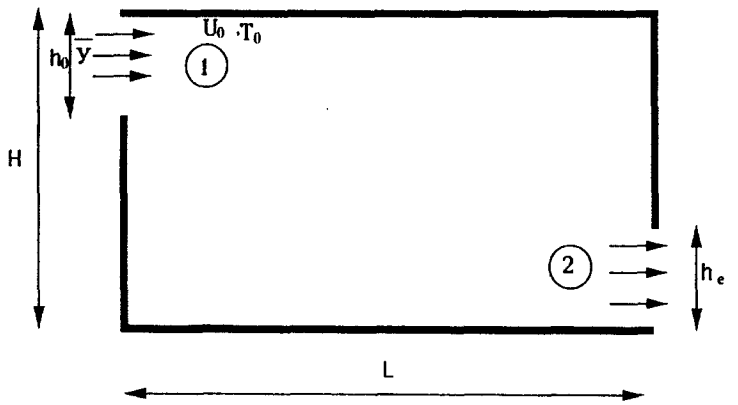

Fig. 1. Flow geometry: (1) inlet; and (2) outlet.

$$u(\text{or } v) = \frac{u'(\text{or } v')}{U_0}, \quad t = \frac{t'U_0}{H}, \quad \theta = \frac{T'-T}{\Delta T},$$

$$\psi = \frac{\psi'}{U_0 H}, \quad \xi = \frac{\xi' H}{U_0}.$$

The initial and the boundary conditions are defined below:

(a) The flow is assumed to be initially at rest with a uniformly distributed temperature. Then $u(x,y,0) = v(x,y,0) = \xi(x,y,0) = 0$, $\psi(x,y,0) = c_1$ and $\theta(x,y,0) = c_2$ with c_1 and c_2 arbitrary constants taken equal to zero.

(b) On rigid non-slip boundary we have: $u = v = 0$ and:

$$\psi = \begin{cases} c_3 \text{ on the upper outline} \\ c_4 \text{ on the lower outline.} \end{cases}$$

c_3 and c_4 are arbitrary constants with $(c_3 - c_4)$ equal to the mass rate flow which enters into the cavity across the opening. Walls are taken as adiabatic or conductive.

(c) At the inlet ($y = \bar{y}$), we impose a uniform profile of both velocity and temperature. Therefore $u(0,y,t) = 1$, $v(0,y,t) = 0 = \xi(0,y,t)$ and $\theta(0,y,t) = 1$.

(d) At the exit from the cavity the temperature distribution and the velocity are unknown. Different conditions can be used as: $U = U_0$, $V = 0$, $\xi = 0$ and $\partial\theta/\partial x = 0$ [2]: a slug flow was used in ref. [7]. Lage *et al.* [9] found that, in a slot ventilated enclosure, the outlet had little influence so zero-mass and heat flux conditions have been used in their study. In this investigation two kinds of outflow boundary condition were taken. In the first, the outflow has been assumed to be parallel. This choice has been determined from experimental flow visualization [10]. The second condition, less restrictive, has been also used, with $\partial(\xi,u,v)/\partial x = 0$. No difference between these results has been observed. The following approximations of ψ and θ have been used:

$$\psi_e = \psi_{el} + \left(\frac{\partial\psi}{\partial x}\right)_{el} \Delta X + O(\Delta X^2) \quad \theta_e = 0.$$

3. NUMERICAL METHOD

The finite difference method has been used for computation of the complete system (1)–(3). A fourth-order implicit compact scheme has been adopted for the resolution of the Poisson stream function equation and a second-order one for the vorticity transport equation. This method using the combination of two finite difference schemes is the so-called combined method and was proposed by Loc and Daube [11] to solve the Navier–Stokes equations and by Safi and Loc [12] to solve coupled problems. Here, the ADI (Alternating Direction Implicit) technique is used to integrate the parabolic equations. This procedure has the advantage that the resulting tridiagonal matrix instead of a matrix with five occupied diagonals can easily be solved by a factorization algorithm.

3.1. *Resolution of the stream function equation*

The equation relating the stream function to the vorticity, equation (1), was set in a quasi-parabolic form and solved by using the following tridiagonal relations between the value of ψ and its first and second derivatives ψ' and ψ'' at three adjacent nodes [13]:

$$\psi'_{i-1} + 4\psi'_i + \psi'_{i+1} = \frac{3}{h}(\psi_{i+1} - \psi_{i-1}) + 0(h^4), \quad (4)$$

$$\psi''_{i-1} + 10\psi''_i + \psi''_{i+1} = \frac{12}{h^2}(\psi_{i+1} - 2\psi_i + \psi_{i-1}) + 0(h^4). \quad (5)$$

By using relation (5), we can write for each step of the $(k+1)$th iteration of the ADI technique the following system:

$$\frac{1}{\Delta\tau_y}\psi_{ij}^{k+1/2} - \left(\frac{\partial^2\psi}{\partial y^2}\right)_{ij}^{k+1/2} = -\xi_{ij}^{k+1} + \left(\frac{\partial^2\psi}{\partial x^2}\right)_{ij}^{k} + \frac{1}{\Delta\tau_y}\psi_{ij}^{k}$$

$$\frac{12}{(\Delta y)^2}(\psi_{i,j-1}^{k+1/2} - 2\psi_{ij}^{k+1/2} + \psi_{i,j+1}^{k+1/2}) - \left[\left(\frac{\partial^2\psi}{\partial y^2}\right)_{i,j-1}^{k+1/2} + 10\left(\frac{\partial^2\psi}{\partial y^2}\right)_{ij}^{k+1/2} + \left(\frac{\partial^2\psi}{\partial y^2}\right)_{i,j+1}^{k+1/2}\right] = 0$$

and

$$\frac{1}{\Delta\tau_x}\psi_{ij}^{k+1} - \left(\frac{\partial^2\psi}{\partial x^2}\right)_{ij}^{k+1} = -\xi_{ij}^{k+1} + \left(\frac{\partial^2\psi}{\partial y^2}\right)_{ij}^{k+1/2} + \frac{1}{\Delta\tau_x}\psi_{ij}^{k+1/2}$$

$$\frac{12}{(\Delta x)^2}(\psi_{i-1,j}^{k+1} - 2\psi_{ij}^{k+1} + \psi_{i+1,j}^{k+1}) - \left[\left(\frac{\partial^2\psi}{\partial x^2}\right)_{i-1,j}^{k+1} + 10\left(\frac{\partial^2\psi}{\partial x^2}\right)_{ij}^{k+1} + \left(\frac{\partial^2\psi}{\partial x^2}\right)_{i+1,j}^{k+1}\right] = 0,$$

where τ_x and τ_y are optimum coefficients of relaxation in the ADI technique [14]. For each line i = constant or j = constant, we have to solve a $3(N-2) \times 3(N-2)$ block tridiagonal system which, in fact, can be easily reduced to an $(N-2) \times (N-2)$ tridiagonal system and dealt with by the factorisation algorithm. Once the new values of $\psi_{i,j}^{n+1}$ of the stream function have been computed by the tridiagonal relation (4), first derivatives $(\partial\psi/\partial x)_{i,j}^{n+1}$ and $(\partial\psi/\partial y)_{i,j}^{n+1}$ are calculated.

3.2. *Resolution of the vorticity transport equation*

A second-order accurate scheme has been chosen to solve equation (2). This choice is motivated by the research on simplicity in checking boundary con-

ditions. In order to overcome the difficulties which are inherent in the treatment of boundary conditions, we use Padé relations [15] to calculate the vorticity at the wall:

$$\xi_p = \frac{12}{h^2}(\psi_{p-1}+\psi_p)+\frac{6}{h}\left[\left(\frac{\partial\psi}{\partial n}\right)_{p-1}+\left(\frac{\partial\psi}{\partial n}\right)_p\right]+\left(\frac{\partial^2\psi}{\partial n^2}\right)_{p-1}+0(h^3).$$

It is important to note that these boundary conditions are always determined from the knowledge of ψ and its derivatives. So a better accuracy for the computation of ψ is needed.

As for the treatment of the Poisson equation an ADI time marching procedure was used for the vorticity transport. Each dimensionless time-step is decomposed into two successive half-steps with a second-order accuracy.

If n is the index of the nth time-step, we have the following expressions:

$$\xi^{n+1/2}_{i,j-1}\left[-\frac{v^{n+1/2}_{i,j-1}}{2h}-\frac{1}{Re\,h^2}\right]+\xi^{n+1/2}_{ij}\left[\frac{1}{\Delta t/2}+\frac{2}{Re\,h^2}\right]+\xi^{n+1/2}_{i,j+1}\left[\frac{v^{n+1/2}_{i,j+1}}{2h}-\frac{1}{Re\,h^2}\right]$$
$$=\frac{Gr}{Re^2}\left(\frac{\partial\theta}{\partial x}\right)^{n+1}-\frac{1}{2h}[(u\xi)_{i+1,j}-(u\xi)_{i-1,j}]^n+\frac{1}{Re\,h^2}[\xi_{i+1,j}-2\xi_{ij}+\xi_{i-1,j}]^n+\frac{\xi^n_{ij}}{\xi t/2},$$

and

$$\xi^{n+1/2}_{i-1,j}\left[-\frac{u^{n+1/2}_{i-1,j}}{2h}-\frac{1}{Re\,h^2}\right]+\xi^{n+1}_{ij}\left[\frac{1}{\Delta t/2}+\frac{2}{Re\,h^2}\right]+\xi^{n+1}_{i+1,j}\left[\frac{u^{n+1}_{i,j+1}}{2h}-\frac{1}{Re\,h^2}\right]$$
$$=\frac{Gr}{Re^2}\left(\frac{\partial\theta}{\partial x}\right)^{n+1}-\frac{1}{2h}[(v\xi)_{i,j+1}-(v\xi)_{i,j-1}]^{n+1/2}+\frac{1}{Re\,h^2}[\xi_{i,j+1}-2\xi_{ij}+\xi_{i,j-1}]^{n+1/2}+\frac{\xi^{n+1/2}_{ij}}{\Delta t/2}.$$

We can note that the components of the velocity u and v are calculated from the values of ψ at time n. Therefore the total order accuracy of this scheme is reduced to $O(h^2)$, $O(\Delta t)$.

3.3. *Resolution of the energy transport equation*

The energy transport equation (3) is of the same type as those of vorticity. Therefore we apply the same treatment as already described.

The Neumann condition of the wall heat flux is discretised at the first order. For every half step, one finally obtains the equation in the x direction:

$$\theta^{n+1/2}_{i,j-1}\left[-\frac{v^{n+1/2}_{i,j-1}}{2h}-\frac{1}{Pe\,h^2}\right]+\theta^{n+1/2}_{ij}\left[\frac{1}{\Delta t/2}+\frac{2}{Pe\,h^2}\right]+\theta^{n+1/2}_{i,j+1}\left[\frac{v^{n+1/2}_{i,j+1}}{2h}-\frac{1}{Pe\,h^2}\right]$$
$$=-\frac{1}{2h}[(u\theta)_{i+1,j}-(u\theta)_{i-1,j}]^n+\frac{1}{Pe\,h^2}[\theta_{i+1,j}-2\theta_{i,j}+\theta_{i-1,j}]^n+\frac{\theta^n_{ij}}{\Delta t/2},$$

and in y direction:

$$\theta^{n+1}_{i-1,j}\left[-\frac{u^{n+1}_{i-1,j}}{2h}-\frac{1}{Pe\,h^2}\right]+\theta^{n+1}_{ij}\left[\frac{1}{\Delta t/2}+\frac{2}{Pe\,h^2}\right]+\theta^{n+1}_{i+1,j}\left[\frac{u^{n+1}_{i+1,j}}{2h}-\frac{1}{Pe\,h^2}\right]$$
$$=-\frac{1}{2h}[(v\theta)_{i,j+1}-(v\theta)_{i,j-1}]^{n+1/2}+\frac{1}{Pe\,h^2}[\theta_{i,j+1}-2\theta_{i,j}+\theta_{i,j-1}]^{n+1/2}+\frac{\theta^{n+1/2}_{ij}}{\Delta t/2}.$$

4. DISCUSSION OF RESULTS

Computational results are obtained for a square cavity with: $H/h_0 = 15$, $h_0 = h_e$ and Reynolds values (based on cavity depth and velocity at the inlet) not exceeding 300. Uniform mesh size with 61×61 nodes was used. Results of the computations are given in the form of contour plots of temperature and stream function at different times.

4.1. *Basic mechanism of the stratification flow*

Establishment of the stratification flow depends on two parameters: the thermal boundary conditions and the Richardson number.

4.1.1. *Effect of boundary conditions.* The incoming flow serves to heat walls and the bounded fluid. When walls are perfectly conductive, this heat is mostly lost from the boundaries. In spite of equal magnitude of inertial and buoyancy forces ($Ri = 1$) the heat front moves in the direction of the exit without a tendency for the fluid to become stratified (Fig. 2, top). When the walls are adiabatic, in the absence of heat loss, the horizontal temperature gradients which tend to form in the vicinity of the inlet are accompanied by changes of density and buoyancy driven motion appears: the fluid then becomes thermally stratified at a shorter time as can be seen in the isotherm contours (Fig. 2, bottom), so only this configuration is presented in the following.

4.1.2. *Critical Richardson number.* Even in the case of adiabatic walls, the stratification does not occur when the buoyancy force is not as important as the inertial force. For $Ri = 0.1$, the thermal front is

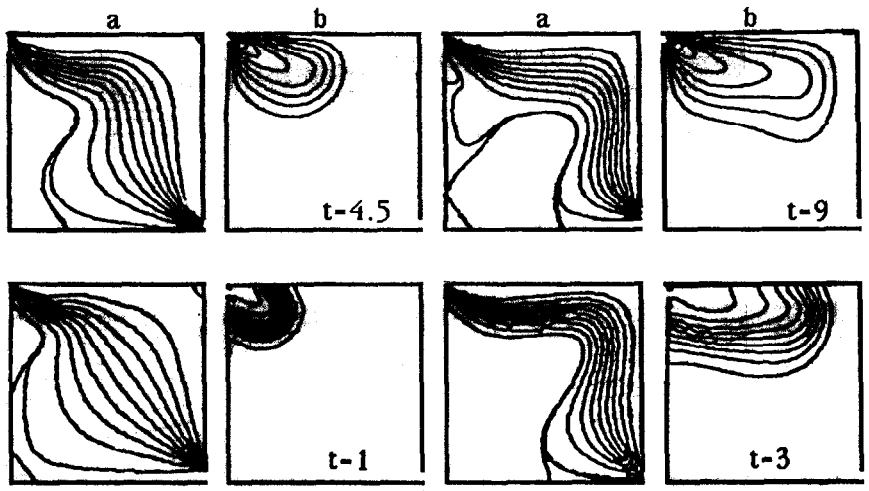

Fig. 2. Effect of boundary conditions: $Re = 300$, $Pe = 214$ and $Ri = 1$: (a) streamlines; and (b) isotherms; conductive walls (top), adiabatic walls (bottom).

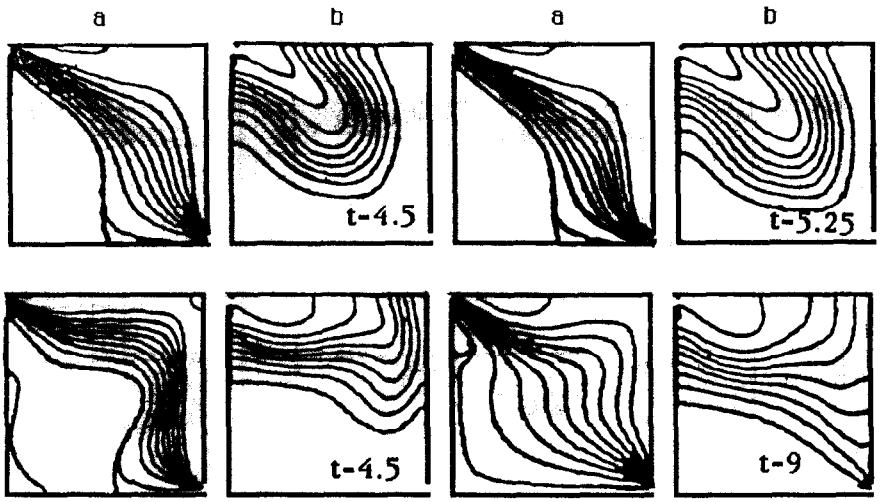

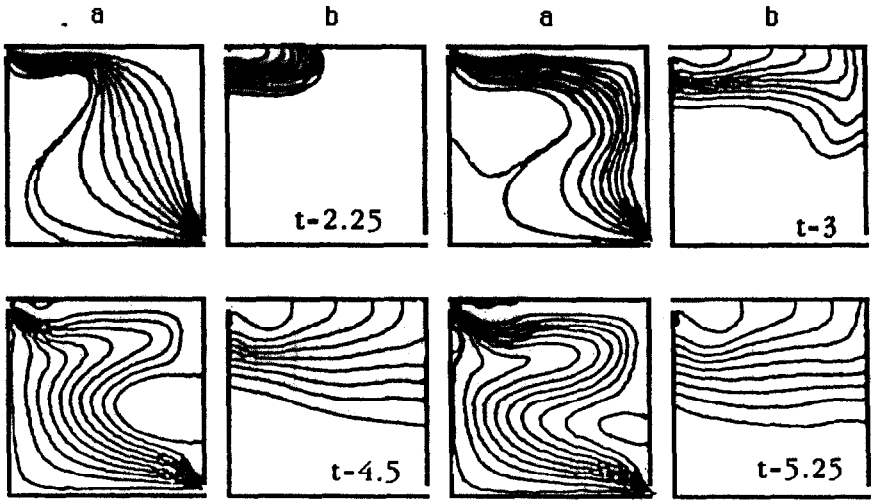

Fig. 3. Effect of the Richardson number: $Re = 300$, $Pe = 214$: (a) streamlines; and (b) isotherms; $Ri = 0.1$ (top), $Ri = 1$ (middle), $Ri = 5$ (bottom).

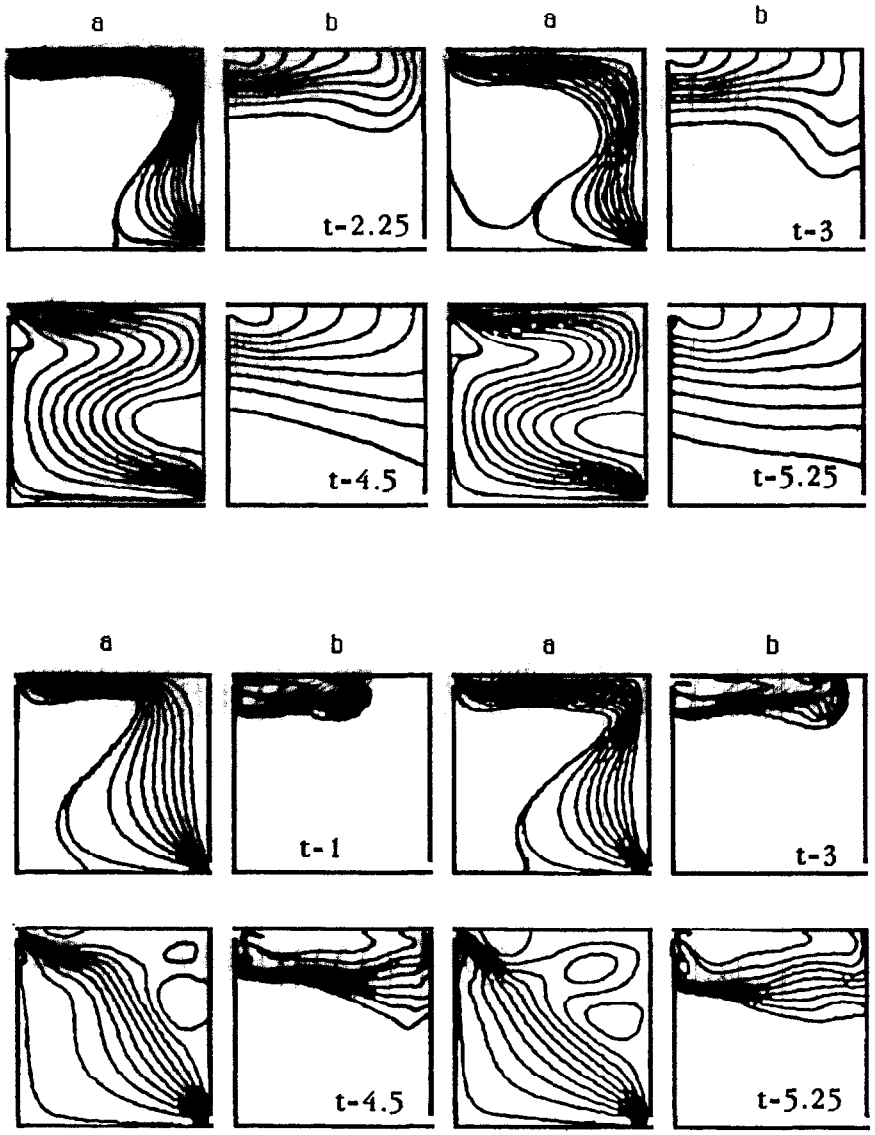

Fig. 4. Effect of the Peclet number: $Re = 300$, $Ri = 5$: (a) streamlines; and (b) isotherms; $Pe = 100$ (top), $Pe = 1650$ (bottom).

pushed by the incoming jet towards the exit, meaning that forced convection is predominant and no stratification appears (Fig. 3, top). As soon as the Richardson value becomes equal to 1, fluid tends to be thermally stratified (Fig. 2, bottom).

The analysis of the flow during the time evolution permits us to understand the basic mechanism of the formation of the stratification. Three steps in the evolution of the flow pattern are observed (Figs. 2 and 3).

First step ($t \leqslant 1$ for $Ri = 1$ and $t \leqslant 0.4$ for $Ri = 5$): the incoming jet entrains fluid and forms an inner closed vortex at each corner of the cavity. At the same time a second vortex is located just down the inlet, while the heat front is located near the inlet.

Second step ($1 < t$ for $Ri = 1$ and $0.8 \leqslant t$ for $Ri = 5$): the two vortices of the left side grow and form a single recirculating zone while the vortex in the upper corner decreases to be smaller than the mesh size. The jet is pushed against the upper edge of the cavity and the associated horizontal thermal propagation increases, providing a vertical thermal gradient.

A secondary vortex (step 3: $t > 3$ for $Ri = 1$ and $t > 2$ for $Ri = 5$) appears in the bottom corner and grows. This one and the main vortex turn in opposite directions exchanging mass flow until they reattach. The two vortices reduce to the little one just under the inlet. At this time the jet is released down and the thermal stratification increases to occupy the whole cavity (Fig. 3).

4.2. *Effect of adimensional parameters*

The three dimensionless parameters which affect the flow appear in the system (1)–(3) and are: *Re*, *Ri*

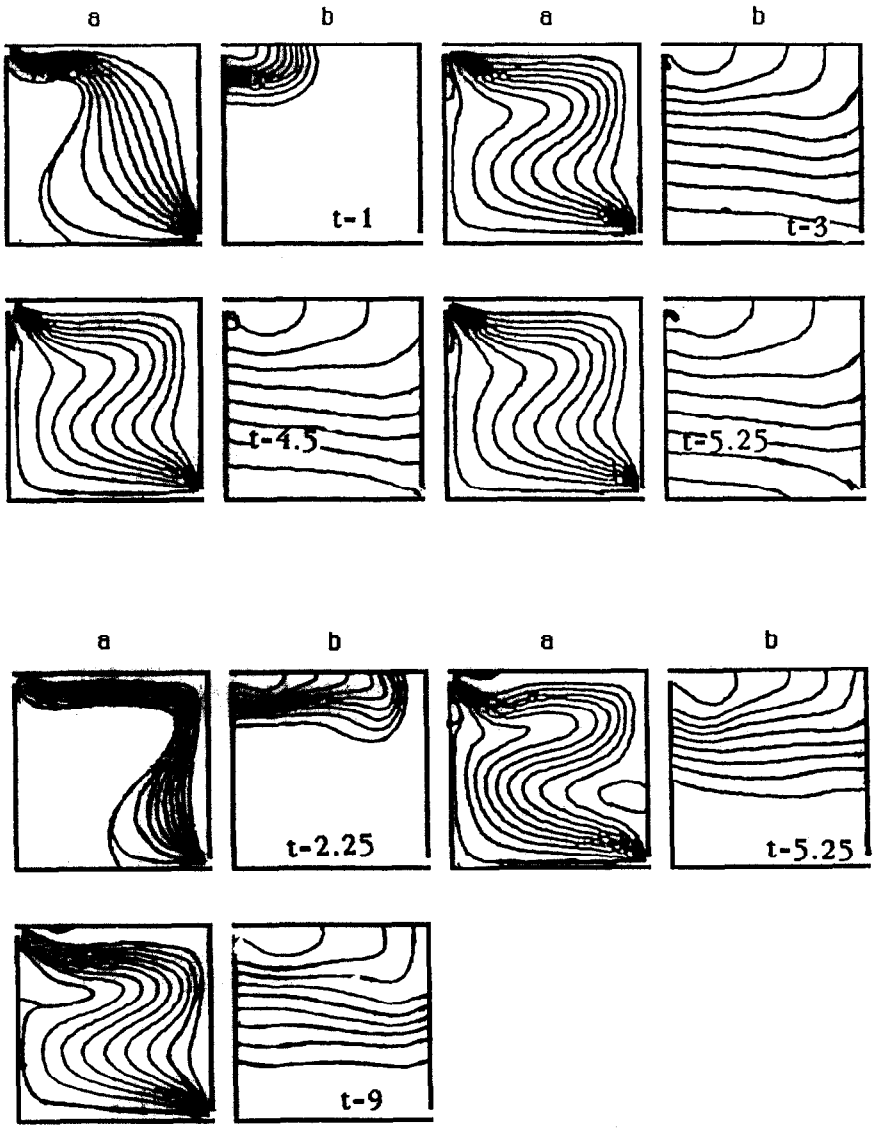

Fig. 5. Effect of the Reynolds number: $Pe = 214$, $Ri = 5$: (a) streamlines; and (b) isotherms; $Re = 150$ (top), $Re = 300$ (bottom).

and Pe. They are, respectively, associated with the diffusion of vorticity, buoyancy force and thermal diffusion.

4.2.1. *Effect of the Richardson number.* In the previous discussion we showed that a critical value of the Richardson number is needed to obtain the stratified regime. Above that value the behaviour of the flow changes.

Calculations were conducted for three values $Ri = 0.1$, 1 and 5 for fixed values of Re and Pe (Figs. 2 and 3). In the two cases the basic mechanism of the stratification is the same but the three steps occur at different times depending on Richardson number value (see Section 4.1.2). Some differences can be pointed out from isotherm contour results.

For $Ri = 1$ (Figs. 2, bottom and 3, middle), the stratification reaches the mid-height of the cavity at $t = 4.5$. Then the isotherms become distorted and directed to the bottom right corner to form, for a longer time $t = 9$, a separation phenomenon: the lowest isotherm of value 0.1 delimits a region where the temperature is uniform and where flow moves toward the exit to be withdrawn.

For $Ri = 5$ (Fig. 3, bottom), isotherms remain parallel up to the vicinity of the outlet and progress slowly through the reservoir. It means that the stratification is more important and more linear than in the last case. Consequently no separation appears. Cold water is pushed toward the bottom to exit from the outlet. The most significant change which can be observed in the isotherm contours is that the flow reverses at the end of the reservoir and forms a closed vortex just on the exit, and then becomes intermittent. This flow, detected by the previous authors, was attributed by Oberkampf [7] to the buoyancy force which tends to keep the warm water near the surface. In fact, this

vortex is the consequence of the selective withdrawal phenomena which occur in stratified mediums when $Ri \geqslant Ri_0$. Yih [16] and Deppler [17] found that $Ri_0 = \pi^2$ for both perfect and inviscid fluids with free surfaces.

4.2.2. *Effect of the Peclet number*. Besides the Richardson number, the Peclet number (or the Prandtl number: $Pe = Pr^*Re$) also takes a predominant part in the stratification process.

Figures 3 and 4 show the pattern flow for three different values of the Peclet number: $Pe = 100$, 214 and 1650 for $Ri = 5$ and 300. We can observe that the flow is stratified for the three values. It means that stratification depends fundamentally on the Richardson number. For the first time steps ($t \leqslant 3$) we have a similar flow in the two cases. For a longer time, flow behaviours are different and we can notice that:

(a) Vortices appear against walls and force the region of main flow to pass near edges. Vortices change in size with time, causing the non-stationarity of the flow. When Pe increases, thermal diffusion is less important, the flow becomes more complex and many vortices appear in the region near the boundaries. This agrees with the results of Sliwinski [18] who noted that the parietal regions are sensitive to the variation of the Richardson number when Pe increases. The transient circulatory motion was found to remain for a longer time before vanishing.
(b) For all that, the thermal field is not disturbed. When Pe increases, thermal gradients become relatively more important as a consequence of increasing of the conductivity. Therefore stratification moves more slowly toward the bottom of the cavity.

4.2.3. *Effect of the Reynolds number*. Figure 5 illustrates the development of the flow and temperature fields for $Ri = 5$, $Pe = 214$ and for two values of the Reynolds number respectively equal to 150 and 300. It is seen that:

(a) Even for low Reynolds values stratification occurs; therefore stratification depends on Ri.
(b) If we compare streamline contours for the two Reynolds numbers at the equal real times (which values for $Re = 300$ are equal to twice the values for $Re = 150$), closer similarities are found. The explanation is that the significant parameters in determining stratification are not Re, but Ri and Pe.

5. CONCLUSION

The numerical simulations used in the present investigation reveal that stratification occurs when the Richardson number is equal to 1. Increasing this value increases stratification but some current reversing appears due to the selective withdrawal. The flow is shown to be strongly dependent on the Richardson and Peclet numbers.

REFERENCES

1. J. A. Duffie and W. A. Beckman, *Solar Energy Thermal Process*. Wiley, New York (1974).
2. A. Cabelli, Storage tanks: a numerical experiment, *Sol. Energy* **19** (1977).
3. G. Abraham, Horizontal jets in stagnant fluid of other density, *J. Hydraulics Division (A.S.C.E)* (July 1965).
4. W. E. Hart, Jet discharge into a fluid with a density gradient, *J. Hydraulic Division (A.S.C.E)* (November 1961).
5. L. Y. Urban, A laboratory investigation of temperature and velocity fields in a stratified cooling reservoir, Ph.D. thesis, University of Texas, Austin (December 1971).
6. Y. Jaluria and S. K. Gupta, Thermal stratification and flow pattern resulting from a heated discharge to a water body, 6th Intl. Heat Transfer Conference, Toronto (1978).
7. W. L. Oberkampf and L. I. Crow, Numerical study of the velocity and temperature fields in a flow-through reservoir, *J. Heat Transfer* (1976).
8. A. Najjam, Thèse de troisième cycle, Université de Poitiers (1982).
9. J. L. Lage, A. Bejan and R. Anderson, Removal of contaminant generated by a discrete source in a slot ventilated enclosure, *Int. J. Heat. Mass. Transfer*. **35**, (1992).
10. M. J. Safi, Visualisation of the recirculating flow in enclosures, 4th Int. Symposium on Flow Visualisation, Paris (August 1986).
11. T. P. Loc and O. Daube, A combined second and fourth order method for the numerical solution of steady and unsteady Navier–Stokes equations, International Conference on Numerical Methods in Laminar and Turbulent flow, Swansea (1978).
12. M. J. Safi and T. P. Loc, Numerical analysis of unsteady mixed convection in an enclosure by a compact hermitian finite difference scheme, 3rd International Conference on Numerical Methods in Thermal Problems, Seattle (August 1983).
13. R. S. Hirsh, Higher order accurate difference solutions of mechanic problems by a compact differencing technique, *J. Comp. Phys.* **19** (1975).
14. E. L. Wachpress, *Iterative Solution of Elliptic Systems*. Prentice-Hall (1986).
15. B. J. Sliwinski *et al.*, Stratification thermal storage during charging, 6th International Heat Transfer Conference, Toronto (1978).
16. C. S. Yih, *Stratified Flows*. Academic Press (1980).
17. W. R. Deppler, Stratification in a line sink, *J. Eng. Mech. Div. Proc, A.S.C.E* (1959).